SPE-192313-MS

Enhancement of challenging prestack land data for improved processing and imaging

Andrey Bakulin, Maxim Dmitriev, Ilya Silvestrov
Geophysics Technology, EXPEC Advanced Research Center, Saudi Aramco

This paper was prepared for presentation at the SPE Kingdom of Saudi Arabia Annual Technical Symposium and Exhibition held in Dammam, Saudi Arabia, 23–26 April 2018.

Abstract

Modern seismic acquisition is trending toward recording high-channel count data with smaller field arrays or single sensors. Reducing the size of field arrays leads to a deterioration of data quality. Many processing steps requiring estimation of prestack parameters become more challenging due to the low signal-to-noise ratio (SNR) of the data. Conventional processing algorithms require estimation of velocities, statics, and surface-consistent scalars and deconvolution operators, and need good prestack data quality. This is rarely the case for land seismic data acquired in arid desert environments of Saudi Arabia with a complex near surface. We present two methods for prestack seismic signal enhancement based on utilization of neighboring traces. The first method, called supergrouping, performs local summation of traces using a global normal moveout correction to align reflected signals. The second approach, called nonlinear beamforming (NLBF), is a data-driven procedure for estimating local moveout directly from the data. We demonstrate the signal enhancement ability of these procedures on synthetic and challenging land seismic data from Saudi Arabia. We show that application of supergrouping and nonlinear beam forming (NLBF) provides significant uplift for various steps of land seismic processing such as deconvolution, estimation of statics, first-break picking, full-waveform inversion (FWI), and imaging.

Introduction

Land seismic data from desert environments suffers from severe contamination originating from complex near-surface scattering. Naturally, every processing step relying on prestack data becomes very challenging to execute. In the past, large source and receiver arrays were used in the field to suppress surface waves and backscattered noise, so that weaker reflected signals could be recorded with a reasonable signal-to-noise ratio (SNR). Modern seismic acquisition is steadily moving toward recording a higher number of channels to increase spatial sampling (Figure 1). High channel counts often come at the expense of using smaller receiver arrays or single sensors. Likewise, a similar tradeoff applies on the source side where increased spatial sampling is accompanied by reduced field source arrays. Theoretically, we get better sampling of signal and noise, and expect to achieve improved imaging results after signal summation. For regions with a complex near surface such as Saudi Arabia such data can be hundreds of terabytes, but with reduced SNR. Signal processing can help, but only if the signal present on each trace is above a certain minimum useful threshold. Unfortunately, much acquired prestack data remains below such a threshold. Figure 2 shows examples of typical single sensor (point-source and point-receiver) data. One can see that prestack signal is extremely weak for both raw data and data after standard preprocessing. Successful imaging relies on estimating many parameters from pre-stack data. If those parameters are not properly estimated, then image quality will be low despite having adequate spatial sampling. In this case, using the signal from neighboring traces to improve the quality of prestack data becomes perhaps the only practical option.

In this study, we propose two methods for enhancing SNR based on local summation of signal. The first method called supergrouping comprises summation of neighboring traces following a global normal moveout correction to align reflected signal. Supergrouping extends conventional group forming to deal with large source/receiver intervals, using simple assumptions and smart summation techniques that prove to work well for field data with low SNR from a variety of different near-surface conditions. A second, more sophisticated approach, called nonlinear beam forming (NLBF) is based on estimation of actual local moveout directly from the data followed by stacking along estimated trajectories (Bakulin et al., 2017). NLBF consists of two steps: estimation of the unknown coefficients (prestack kinematic attributes) using semblance optimization and weighted summation of seismic events along the estimated surfaces similar to CRS (common reflection surface) or multi-focusing techniques (Baykulov and Gajewski, 2009; Berkovitch et al., 2011; Buzlukov and Landa, 2013). In this paper, we briefly describe these two techniques and demonstrate applications to various seismic datasets from Saudi Arabia.

Supergrouping

Supergrouping is based on local summation of nearby traces to enhance SNR. It is very similar to conventional group forming in that traces are summed within the group, but there are some differences. Since there is no practical way to align the reflected events of interest in the field, conventional shot/receiver groups require very fine sampling so that summation does not smear the signal. The spatial sampling of modern high-channel count data or single sensor usually remains significantly larger than is required for conventional field array forming. This creates a challenge for seismic processing that can no longer rely on large field arrays or conventional group forming. Supergrouping is typically applied to input data that has already been recorded with source/receiver arrays (grouped) hence the use of the term supergrouping. Supergrouping can be implemented in the source or receiver domain, or any other domain. For example, to construct a receiver group we find and sum all traces around reference traces of each common shot gather (Figure 3). Likewise, source supergrouping can be similarly performed in the common-receiver domain. In all examples presented here, the output trace geometry is identical to the input, although regular coarser geometry may also be output for some processing steps. Therefore, this process could be thought of as a sliding spatial window where an enhanced trace is output at the “central” location of the supergroup aperture. Trace summation itself can be done using different methods. Similar to field arrays, we can use straight or simple summation. While simple summation is robust and fast, it has three main limitations. First, it does not account for moveout differences (time shifts with respect to the signal recorded by reference trace). Second, it assumes that trace amplitudes are well balanced inside stacking window, i.e., it has approximate equal amplitudes. Third, individual traces inside each supergroup may be recorded over quite different near-surface conditions (variable source and receiver coupling, changing environmental noise etc.) and can have different statics and variations of waveform. While these limitations are uncorrectable using field source and receiver arrays, they can all be compensated for during supergrouping in processing. To address the first limitation, we apply supergrouping after normal moveout correction (NMO) using generally available preliminary velocity information. It allows us to preserve signal at higher frequencies and use larger summation apertures that are impossible to use in conventional group forming. The second limitation is addressed by using diversity stacking (Martinez et al., 1993) that weights each trace by its smoothed envelope before summation, while the final sum is then normalized by the sum of the original weights. Diversity stacking helps to prevent high-amplitude noise bursts from smearing to adjacent traces. More advanced weighted summation (Neklyudov et al., 2017) allows to handle intra-array statics and waveform variations inside the supergroup. The weights apply special amplitude and phase corrections for each frequency component of the gathers used in forming a supergroup.

We propose to use supergrouping as an efficient way to achieve desirable SNR for optimal parameter selection for each prestack processing step. Figure 4 shows a typical workflow for processing land seismic data. To process and image seismic data, we have to be able to find this signal, apply appropriate corrections, remove noise and then image. Processing algorithms utilized today largely rely on good pre-stack signal to be present on the bulk of the traces, which is often not the case with modern data acquired with smaller arrays or single sensors. For instance, surface-consistent deconvolution analyzes prestack events within an appropriate time window and assumes they represent reflected signal. Likewise, surface-consistent scaling looks at prestack amplitude variations, also assuming they are from reflections. If these assumptions are violated, then parameters for filtering, scaling, statics and velocity analysis are poorly estimated and result in poor imaging. Each processing step may demand a different level of enhancement. Supergrouping provides the noise suppression power of large field arrays and allows task-specific flexibility. Let us examine how smart supergrouping can help at various stages of seismic data processing.

Surface-consistent processing: 2D point-source point-receiver land data

Point-source point-receiver data, if high density, is often assumed to be the ultimate acquisition design. In a desert environment such data often contains little visible signal. Here we examine 2D point-source and point-receiver data from northern Saudi Arabia and compare results from conventional single-sensor processing vs. processing involving supergrouping with relatively small group size (seven receivers inline). First, let us review surface-consistent deconvolution and residual statics. Deconvolution operators are derived from autocorrelations shown in Figure 5. Those obtained from the supergrouped data are without the extreme trace-to-trace variations that are likely caused by near-surface noise rather than actual variation in reflection signature (Figures 5a and 5b). For wavelengths of 100 m or more, wave propagation dictates that we should not see large waveform changes between receivers that are 10 m apart. Therefore, the observed rapid variations are probably a result of near-surface scattering and recorded noise. Likewise, estimated residual shot statics for single-sensor data often exceed user-specified bounds suggesting that prestack traces are simply lacking enough signal to determine accurate values based on simple cross-correlation (Figure 5c). On supergrouped data, statics estimates cover a narrower time range with a smaller standard deviation suggesting the results are more stable. Comparing stack images in Figures 5d and 5e clearly suggests that these parameter improvements (statics, velocities, etc.) after supergrouping are helpful. Supergrouped data show both deep and shallow events with better continuity as well as exhibit a more stable wavelet along the line. In this case, we use supergrouped data for further processing since we feel that single-sensor data does not meet the minimum signal requirement for reliable imaging.

Automatic first-break picking

For modern data with smaller field arrays, even the strongest arrivals from refracted waves may lack sufficient SNR needed for reliable and accurate first-break picking and near-surface modeling. For large 3D surveys with high trace density (total data size can be hundreds of terabytes), automatic first-break picking is essential to handle the data volume and some minimum SNR is required for these algorithms to work. Here we show examples of data enhancement using supergrouping for high-channel data with small field arrays (nine geophones per receiver group and two vibrators per source array). Source spacing is on a 125 m by 25 m grid and receivers are on a 25 m by 125 m grid. Despite good spatial sampling prestack data has very low SNR. Figure 6 shows a common-shot gather and corresponding picks (blue dots) using a standard processing workflow. One can see that picking fails in many places, especially for far offsets where SNR is typically lower. As a consequence, tomographic inversion and resulting statics will have large errors and uncertainty. To improve data quality we use supergrouping in the common-offset domain using CDP coordinates (cdp_x, cdp_y). When we apply supergrouping using a 400 by 400 m aperture we obtain very good improvement for both middle and far offsets (Figure 6, red dots). Despite ignoring surface azimuth, we found that refracted events were not damaged. While we may lose some details, they represent middle and high frequency statics. These statics can be estimated using an iterative approach by progressively going from large to small supergrouping and using obtained picks from previous estimation as a guide.

Enhancement of low frequencies for FWI

Full-waveform inversion (FWI) is a data-driven approach growing in popularity aimed at estimating subsurface velocities by minimizing the misfit between measured and modeled data. A lack of low frequencies in seismic data is a central issue in FWI (Virieux et al., 2009). Due to strong nonlinearity, the natural way to apply FWI on bandlimited data is to use a multi-scale hierarchical approach proceeding sequentially from low to higher frequencies. The key element of this multi-scale strategy is availability of low frequencies such as 1.5 to 3 Hz that are at the edge of the spectrum of conventional broadband data. Low frequencies help to avoid the cycle-skipping problem when comparing waveforms in FWI prevent convergence to a local minimum. Obtaining such information from broadband land data in an arid desert environment represents a significant challenge because of poor SNR. We demonstrate the effect of supergrouping on a 3D broadband land seismic dataset from Saudi Arabia acquired using a nonlinear sweep from 2 to 90 Hz. Receivers are spaced every 50 m inline and 250 m in the crossline direction. Likewise, sources are spaced every 50 m cross-line (orthogonal to receivers) and 250 m inline. Note that each receiver station is actually a small geophone group of 25 elements and each source station represents linear array of three vibrators at 12.5 m spacing in the inline direction. We perform basic preprocessing of raw data comprising suppression of noisy traces with high amplitudes and linear noise removal for groundroll. One can see that that a significant amount of noise remains after filtering (Figures 7a and 7c). Figure 7b and 7d shows supergrouped data using a two-dimensional symmetric 5x5 shot and receiver supergroup (200 m for shots in crossline direction and 200 m for receivers in inline direction) followed by common-offset summation in the inline direction using five shots. SNR was greatly improved both in time and frequency domains, which will be critical to allow frequency-domain FWI to work. Supergrouping with the same shot and receiver group size was also tested on synthetic data and shown to fully preserve refracted and reflected waves of interest up to 8 Hz, while suppressing groundroll and shear waves. For synthetic data in acoustic media, supergrouped traces and point source/receiver responses were very similar, verifying that events of interest are preserved at low frequencies on all traces within the summation aperture.

Improving repeatability for 4D seismic monitoring

Time-lapse or 4D monitoring of onshore reservoirs in a desert environment represents a challenging geophysical task. Land seismic data typically has low SNR and requires dedicated processing. To extract reliable 4D signal associated with changing reservoir properties we should have excellent repeatability between different surveys. Here we demonstrate supergrouping for improving data repeatability for a permanent monitoring system with around 1000 point receivers buried at depth of 70 m (Bakulin et al., 2016). Vibroseis sources are located on the surface and sampled on a grid of 10 by 10 m. Figures 8a and 8b show a common-receiver gather before and after standard processing. One can see that processing did an excellent job in cleaning up the noise and highlighting reflections. For data enhancement we performed 7x7 shot supergrouping (70x70 m) after NMO correction as an additional processing step. Clearly, supergrouping helped to boost SNR by stacking nearby shots. We use normalized root-mean-square (NRMS) to measure repeatability between seismic traces (Bakulin et al., 2016). Figure 9 shows the progression of the stack repeatability measured around a target horizon through the main steps of the processing sequence. We observe that supergrouping has approximately halved all the NRMS estimates in comparison with standard processing. Since lower NRMS is closely related to better signal-to-noise ratio, we conclude that supergrouping arrays can deliver additional suppression of coherent and random noise that is not included in a simple single-sensor imaging process. Supergrouping is now one of the cornerstone elements of 4D processing for land time-lapse data (Bakulin et al., 2016).

Nonlinear beamforming

Supergrouping of nearby traces applied after NMO corrections proved as a simple and practical tool to enhance SNR for big high-channel count and single sensor data. Application of NMO corrections prior to supergrouping allows us to handle larger spatial separation between traces. Supergrouping uses a simple assumption about global hyperbolicity of the reflections, and stacking is always done along hyperbolic NMO curves (Figure 10a). In the presence of a complex near surface or subsurface, the assumption of global NMO breaks down. Buzlukov et al. (2010) and Buzlukov and Landa (2013) proposed an approach for enhancing prestack data based on searching for locally coherent events in the data and partial summation along the estimated trajectories. This can be considered as a delay-and-sum beamforming method. Unlike conventional beamforming (slant stack), the time-delay in this approach is a nonlinear function of distance. Further advances were achieved by Buzlukov et al. (2010), Buzlukov and Landa (2013) and Xie and Gajewski (2017). Building on this earlier work we introduce nonlinear beamforming (NLBF) for enhancing challenging pre-stack land seismic data with low signal-to-noise ratio caused by strong near-surface scattering. NLBF can be written as follows:

$$u(x_0, y_0, t_0) = \sum_{(x,y)\in B_0} w(x,y)u\big(x, y, t_0 + \Delta t(x,y)\big), \quad (1)$$

where $u(x_0, y_0, t_0)$ represents a seismic trace with spatial coordinates x, y and time t. The coordinates of the output trace after the beamforming procedure are given by x_0, y_0 and t_0. The summation is done over local region B_0 around the output trace in the x-y domain along trajectory with moveout $\Delta t(x,y)$ (Figure 10b). The beamforming weights $w(x,y)$ are used to preserve signal energy and to suppress noise. In the following examples, we use simple fold normalization, but more sophisticated approaches can be adopted. Here we assume that the travel-time surfaces can be locally approximated by a second order surface as follows:

$$\Delta t(x,y) = t(x,y) - t_0(x,y) = A\Delta x + B\Delta y + C\Delta x\Delta y + D\Delta x^2 + E\Delta y^2, \quad (2)$$

where parameters $\Delta x = x - x_0, \Delta y = y - y_0$ and parameters A, B, C, D, E are unknown beamforming parameters that are estimated using coherency analysis. Due to the computational demand of simultaneous estimation of five parameters we follow a similar approach to Hoecht et al. (2009) and first perform a two-parameter scan for A and D, followed by another scan for B and E. Finally, we fix these four coefficients and search for an optimal value of C. This scheme provides reasonable trade-off between accuracy and performance. The beamforming coefficients have particular physical meaning in models of mild complexity. For example, the A and D coefficients correspond to slope and curvature of events in the x-t domain (section of x-y-t cube along the y-axis). Similarly, the B and E coefficients define slope and curvature of events in the y-t domain (section of x-y-t cube along x axis). The mixed coefficient C couples the two domains. After the parameter estimation step is done, we perform local summation along estimated trajectories using operator-oriented approach (Hoecht et al. 2009; Bakulin et al. 2017). In a similar way to supergrouping, we apply global NMO corrections prior to enhancement to minimize the possible dip and curvature ranges for searching the coherent seismic events. This provides a significant reduction in calculation time of the most time-consuming estimation procedure. Note that NMO velocity does not need to be very accurate because we can control the possible search range of dips and curvatures with respect to NMO corrected gathers.

Synthetic test

To validate performance of the local summation we compare depth migrated images using synthetic data generated for the Sigsbee model similar to one presented in Baykulov and Gajewski (2009). Local data summation was done in the CMP-offset domain. Figures 11a and 11b show a comparison of Kirchhoff depth migrated data after supergrouping and NLBF for a stacking aperture 100 ft. One can see that for such a relatively small aperture we do not observe much difference between the seismic images. In contrast, larger apertures (500 ft) used in supergrouping result in significant smearing of both faults and dipping structures, whereas NLBF images remain largely unaffected with some smearing of the faults only (Figures 11c and 11d). For less complex models, these distortions are expected to be much less. These tests shows that NLBF and supergrouping with small apertures can be used not only for data enhancement, but also for improved seismic imaging on challenging data.

Enhancement of 2D point-source point-receiver land data

We apply nonlinear beamforming to the same point-source point-receiver land seismic data from Saudi Arabia described in previous sections. As an input for NLBF we use data after small receiver supergrouping (7 receivers). After supergrouping, reflections start to become visible (Figure 12b), albeit very weak. Enhancement of the data using NLBF was done in the CMP-offset domain. NLBF with a summation aperture of 150 m reveals stronger and more coherent events (Figure 12c). Figure 13 shows how velocity semblance panels after supergrouping are compared to the nonlinear beamforming result. The initial velocity that was used as a guide is shown as a black line. In this example, the velocity and dip of events during the automatic coherency scan are perturbed up to 10%. Even though this was done locally for each point in the CMP-offset section lying on 150x100 m grid, we observe a clear improvement in the quality of the semblance maxima now clustering around the guide velocity. Nonlinear beamforming employs massive partial stacking from neighboring midpoint positions and reveals reflection events not visible in the original data. We also note that the beamforming and supergrouping also partially suppresses multiples (white ellipse in Figure 13c). Figure 14 shows corresponding post-stack migrated images before and after NLBF enhancement. One can see good improvement for both shallow and deep sections. We expect to obtain further improvements after applying the Enhance-Estimate-Image approach (Bakulin and Erickson, 2017) involving deriving new velocities and other pre-stack parameters using the enhanced data and iterative imaging with new parameters. This will be investigated in future studies.

Conclusions

We present here supergrouping and nonlinear beamforming approaches for enhancement of prestack seismic data using local summation of the traces. Both techniques are rapidly becoming an essential part of the seismic processing toolbox especially in the areas with complex near surface and where seismic data has low SNR. Supergrouping enhances the reflected signal based on global hyperbolic NMO corrections and can be especially efficient for areas with simple geological structure. By adjusting the group size, one can set a different level of enhancement for each processing task. For instance, strong enhancement with large supergroups may be perfectly acceptable for velocity analysis, while milder enhancement can be used for deriving residual statics with small enhancements for final imaging. NLBF goes further and estimates actual moveout corrections directly from the data without prior knowledge of the velocities. It is free from the hyperbolic assumptions of supergrouping algorithm and is based on a general local second-order approximation of traveltimes. NLBF enables larger summation apertures resulting in stronger enhancement, although it requires significant computational power for parameter estimation and local summation of huge volumes of seismic data. Both NLBF and supergrouping allow us to greatly enhance the quality of pre-stack data critical for derivation of processing parameters and successful imaging of modern land 3D seismic data.

Acknowledgments

The authors thank Saudi Aramco for the opportunity to publish this paper. We are grateful to Saud Zainaldin, Robert Wilson, Pierre Leger, Pavel Golikov, Victor Dolgov and Robert Smith from Saudi Aramco for support of this work and valuable comments. We thank Dmitry Neklyudov, Maxim Protasov and Kirill Gadylshin from Institute of Petroleum Geology and Geophysics for their help and fruitful discussions.

References

Baykulov, M. and Gajewski D. 2009. Prestack seismic data enhancement with partial common-reflection-surface (CRS) stack. Geophysics, 74, V49-V58.

Berkovitch, A., Deev, K. and Landa, E. 2011. How non-hyperbolic MultiFocusing improves depth imaging. First Break, 29, 103-111.

Buzlukov V., Baina R. and Landa E. 2010. Prestack Data Enhancement Using Local Traveltime Approximation. 72nd EAGE Conference and Exhibition, 372-376.

Buzlukov, V. and Landa, E. 2013. Imaging improvement by prestack signal enhancement. Geophysical Prospecting, 61, 1150-1158.

Bakulin, A., Golikov, P., Dmitriev, M., Dolgov, V., and Neklyudov, D. 2016. Application of supergrouping to land seismic data in desert environment. 86th Annual International Meeting, SEG Technical Program Expanded Abstracts, 4649-4653.

Bakulin, A., Smith, R., Jervis, M., Saragiotis, C., Al-Hemyari, E. and Alramadhan, A. 2016. Processing and repeatability of 4D buried receiver data in a desert environment. SEG Technical Program Expanded Abstracts, 5405-5409.

Bakulin, A., and Erickson, K. 2017. Enhance-estimate-image: New processing approach for single-sensor and other seismic data with low prestack signal-to-noise ratio. 87th Annual International Meeting, SEG Technical Program Expanded Abstracts, 5001-5005.

Bakulin, A., Silvestrov, I., Dmitriev, M., Golikov, P., Neklyudov, D., Protasov, M., Gadylshin, K. and Tcheverda, V. 2017. Nonlinear beamforming for enhancing prestack data with challenging near surface or overburden. SEG Technical Program Expanded Abstracts, 4996-5000.

Hoecht, G., Ricarte, P., Bergler, S. and Landa, E. 2009. Operator-oriented interpolation. Geophysical Prospecting 57, 957-981.

Martinez, R.D., Masters J.R., and Fryar D. 1993. Prestack noise attenuation using the diversity Tau- p transform. 63rd Annual International meeting, SEG Technical Program Expanded Abstracts, 1187-1190.

Neklyudov D., Bakulin, A., Dmitriev, M., Silvestrov I. 2017. Intra-array statics and phase corrections obtained by beamforming in the Short-Time Fourier Transform domain: Application to supergrouping. 87th Annual International Meeting, SEG Technical Program Expanded Abstracts, 4991-4995.

J. Virieux, S. Operto. 2009. An overview of full-waveform inversion in exploration geophysics. Geophysics, 74 (6), pp. WCC1-WCC26.

Xie Y. and Gajewski D. 5-D interpolation with wave-front attributes. Geophysical Journal International, 211, 897-919.

Figures

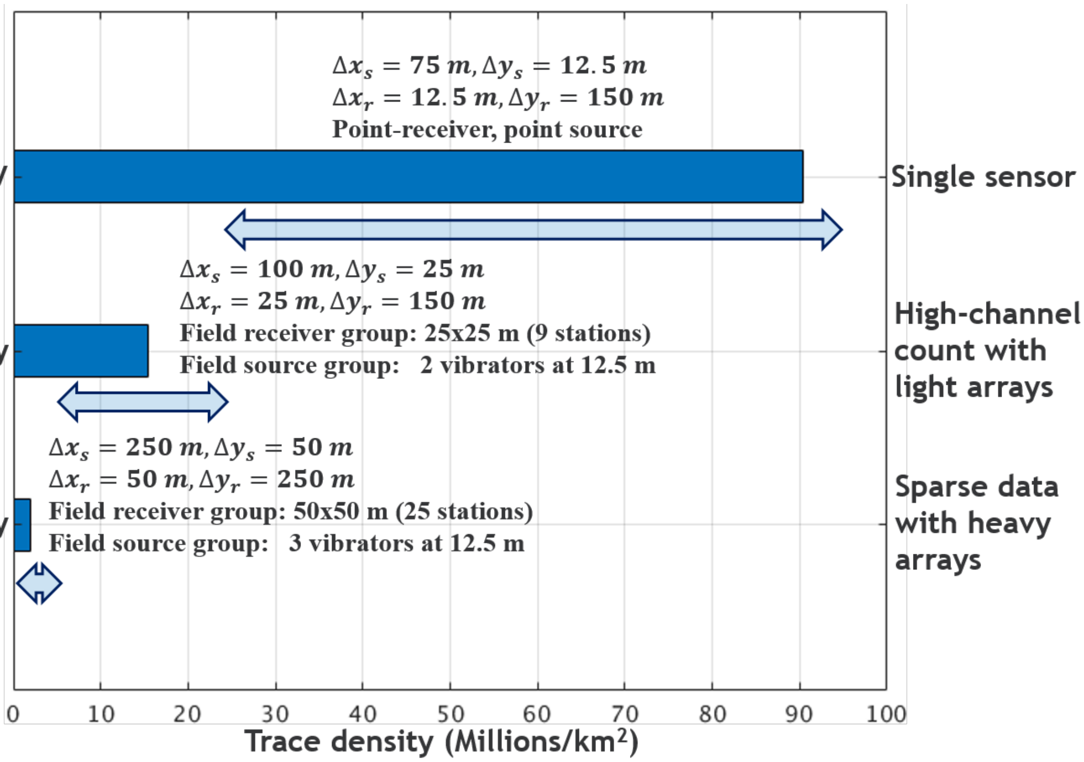

Figure 1 – Examples of acquisition geometries illustrating the trend to increase trace density. Observe that in practice this is accompanied by a reduction in field source and receiver arrays.

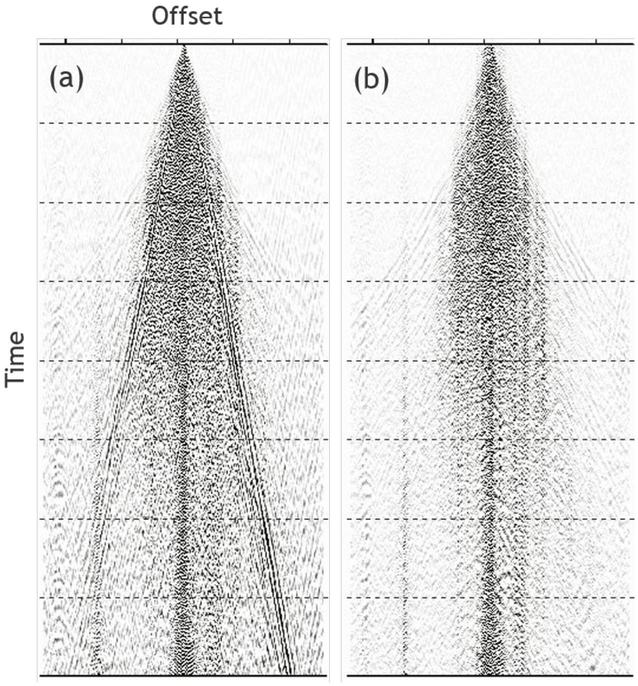

Figure 2 – Single-sensor data as recorded in the field (a) before and (b) after standard noise removal. Observe low signal-to-noise ratio on (b) insufficient for standard time processing.

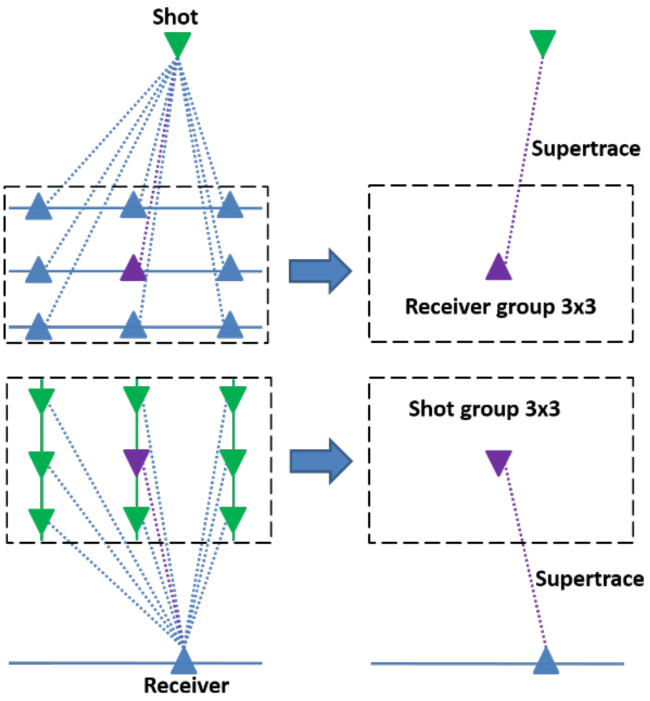

Figure 3 – Scheme explaining supergrouping for 3D data.

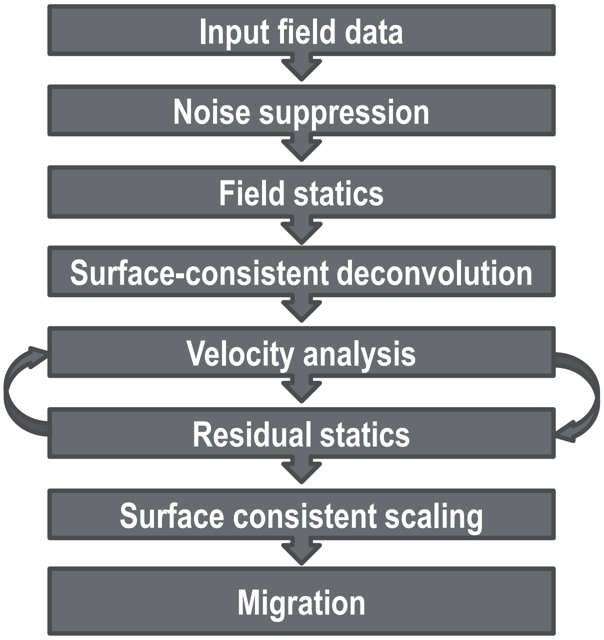

Figure 4 – A generalized land seismic data processing flow.

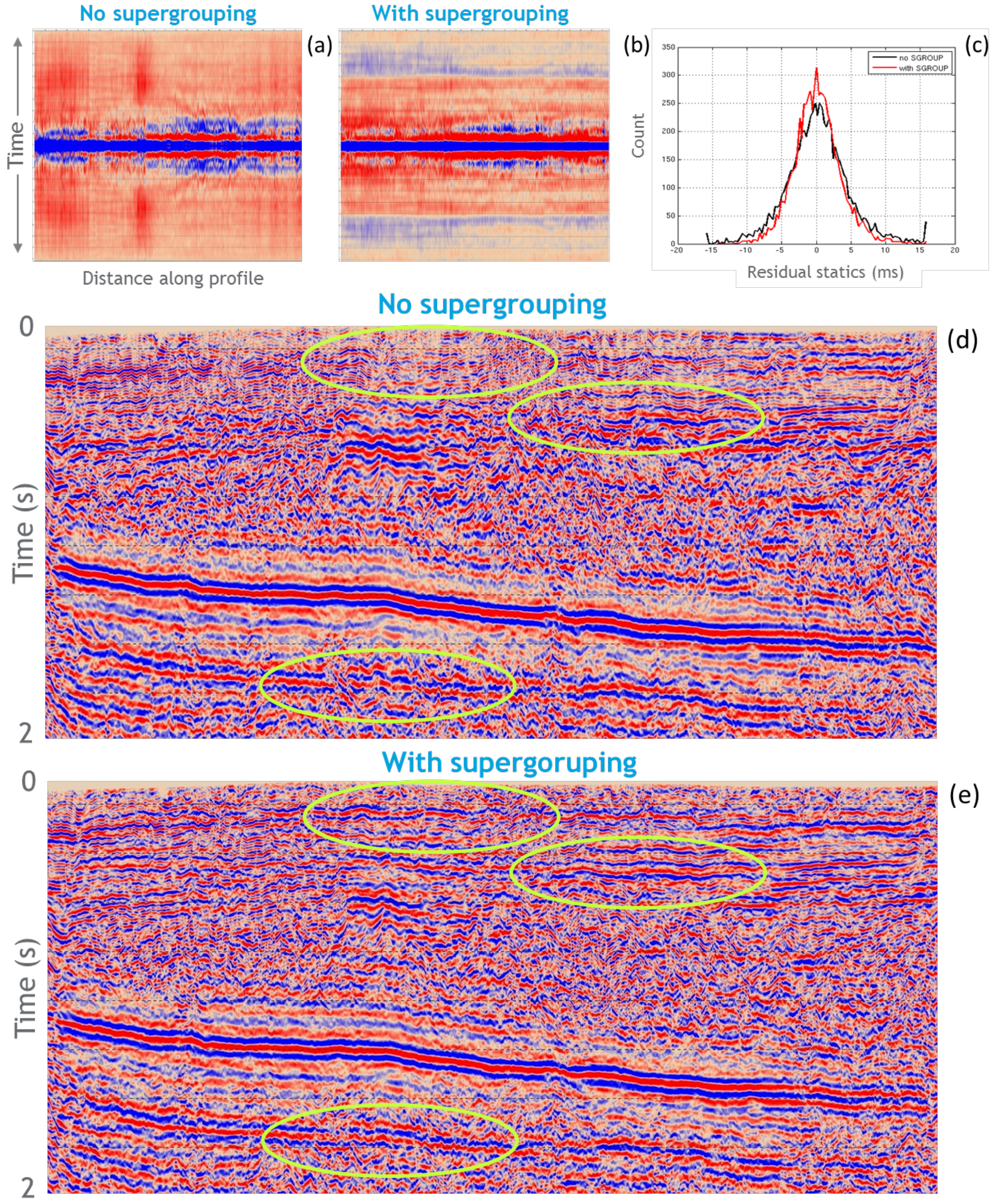

Figure 5 – Surface-consistent processing for challenging point-source, point-receiver 2D data. Summed autocorrelations (a) before and (b) after supergrouping with seven receivers (7x1) show that input to deconvolution is cleaner and less contaminated when supergrouping is applied. Residual statics are shown (c) with and without supergrouping. Stacked sections are shown (d) without supergrouping for statics and (e) after residual statics are computed on supergrouped data.

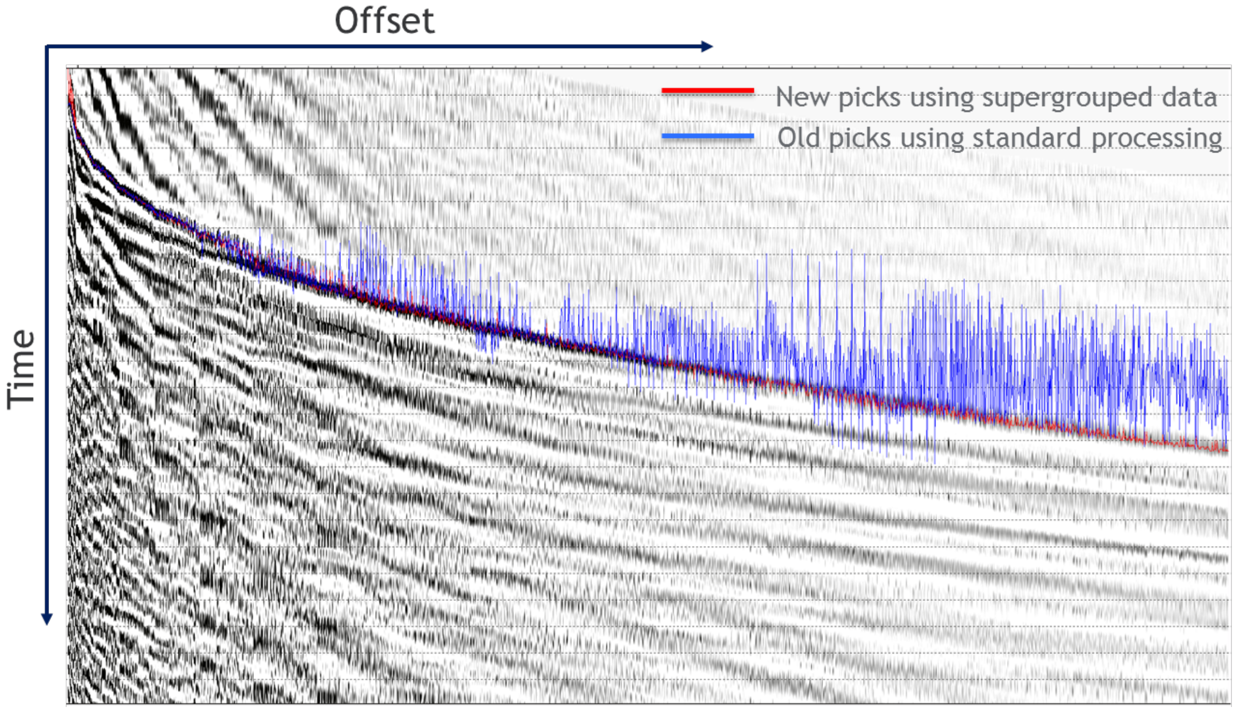

Figure 6 – First break picks obtained with automatic picker using data after standard processing (blue) and supergrouped data in common offset domain (red). Observe more robust and consistent picks for supergrouped data.

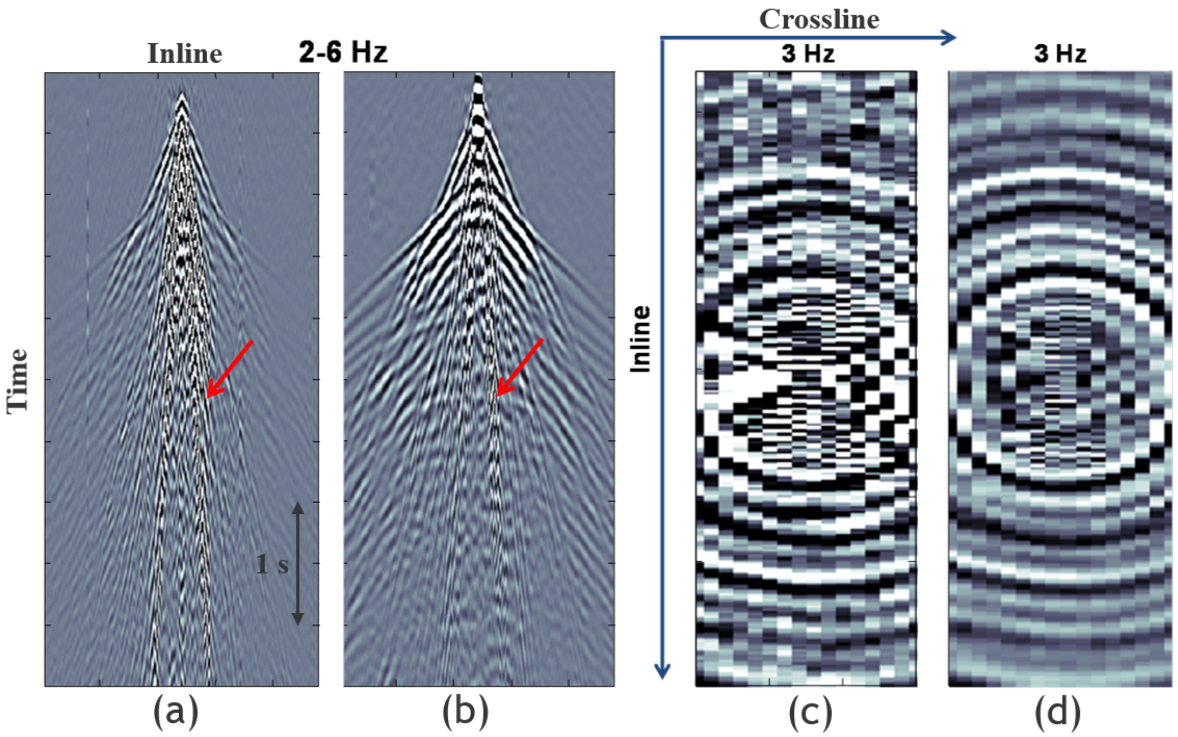

Figure 7 – Broadband field data for the near cable bandpass filtered to 2-6 Hz showing (a) pre-processed common shot gather, (b) the same gather after symmetric supergroup 5x5 (200 m for shots in crossline direction and 200 m for receivers in inline direction) followed by common-offset summation in the inline direction using five shots, (c) pre-processed input data in frequency domain and

(d) the supergrouped data in the frequency domain.

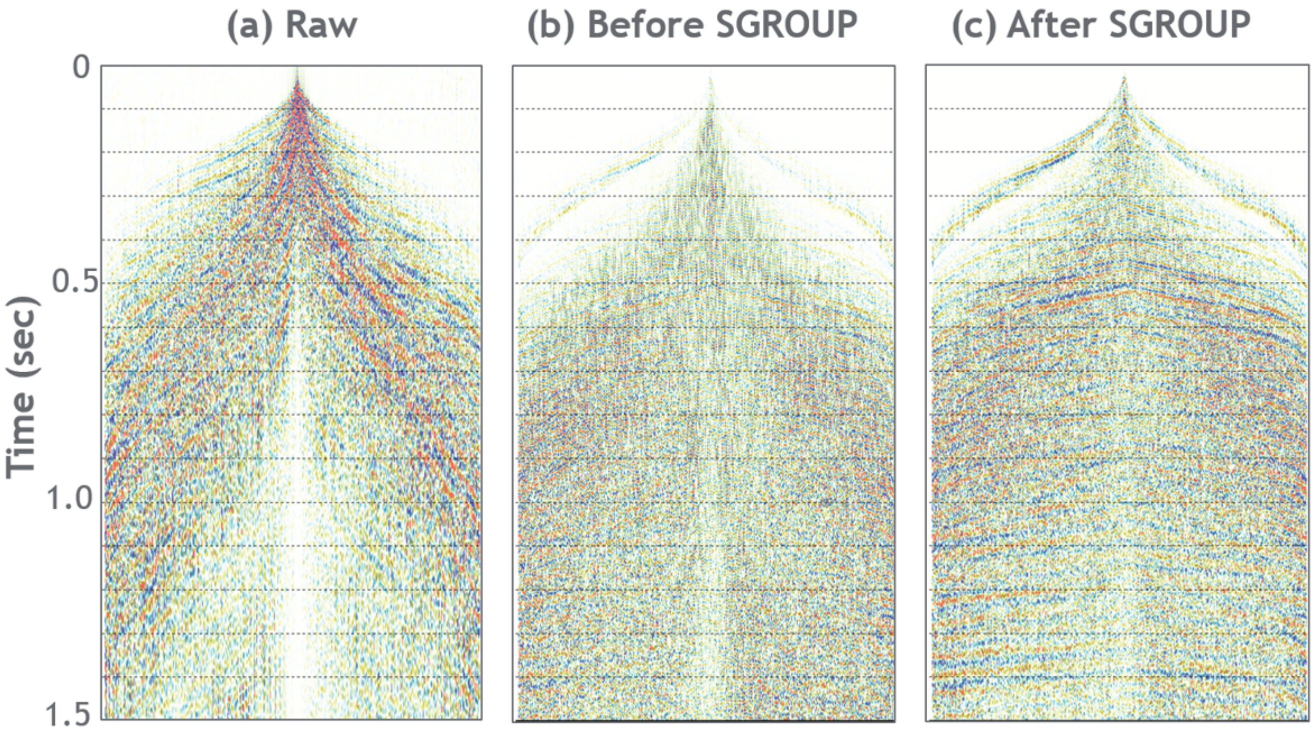

Figure 8 – Prestack common-receiver gather recorded with buried receivers in 4D monitoring project: (a) before processing, after processing (b) without and (c) with supergrouping. Observe clear improvement of SNR for supergrouped data.

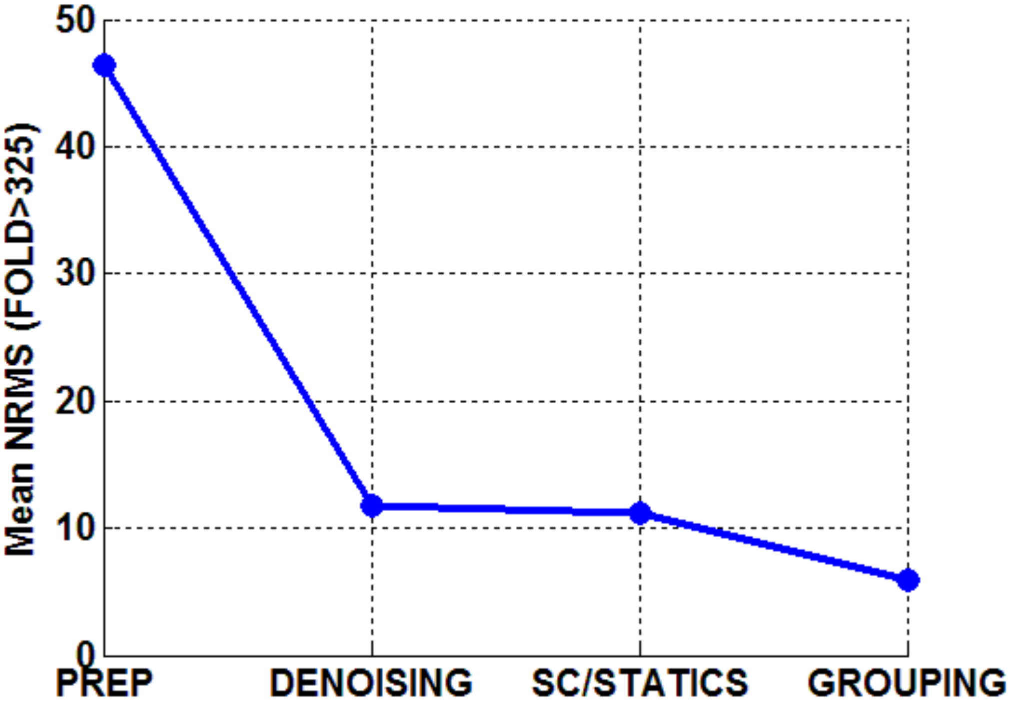

Figure 9 – Progression of NRMS stack repeatability (mean value measured over high-fold areas) throughout the processing sequences: noise removal, multi-servey survey consistent processing, residual statics, and supergrouping. Observe that

supergrouping reduces NRMS by 50 % and greatly improves repeatability of 4D images.

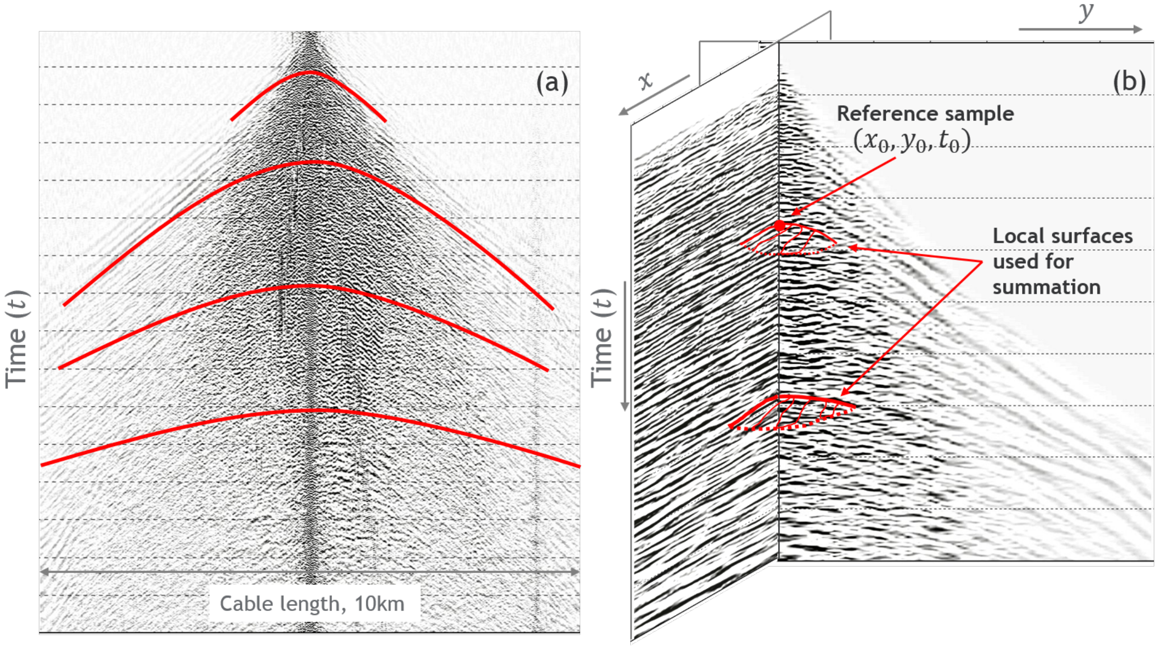

Figure 10 – Trajectories used for summation for (a) supergrouping and (b) nonlinear beam forming approaches.

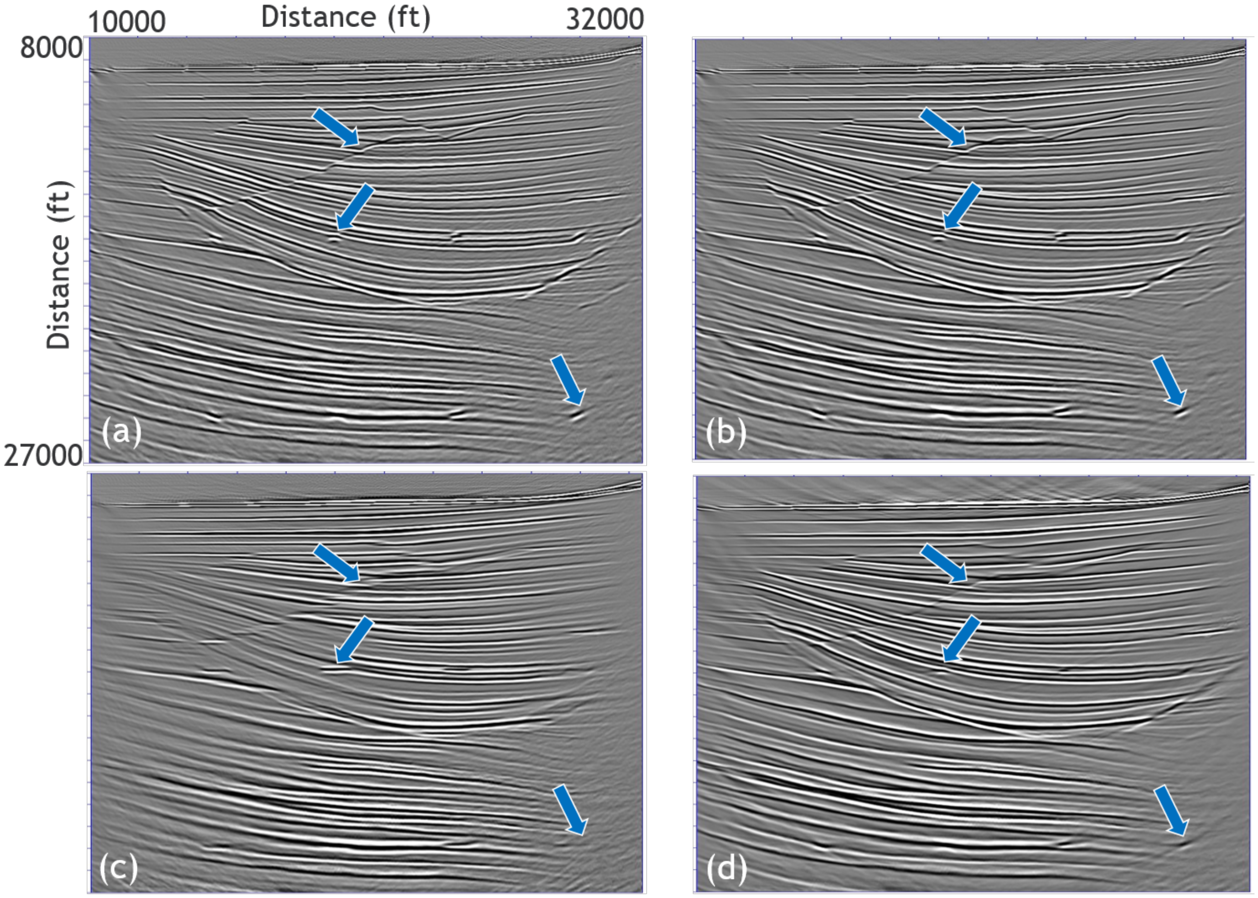

Figure 11 – Depth-migrated images using the true Sigsbee model for different stacking apertures: (a) supergrouping 100 ft, (b) NLBF 100 ft, (c) supergrouping 500 ft, and (d) NLBF 500 ft.

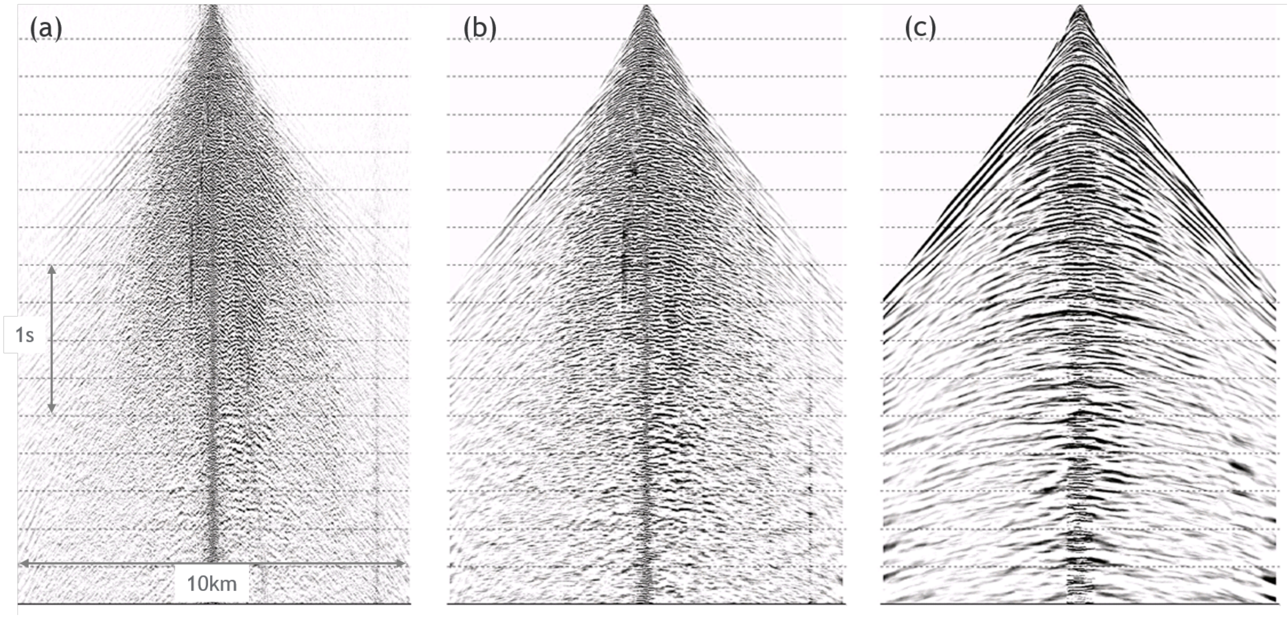

Figure 12 – Common-shot gathers for (a) original data, (b) data after 1x7 supergrouping, and (c) data after nonlinear beamforming.

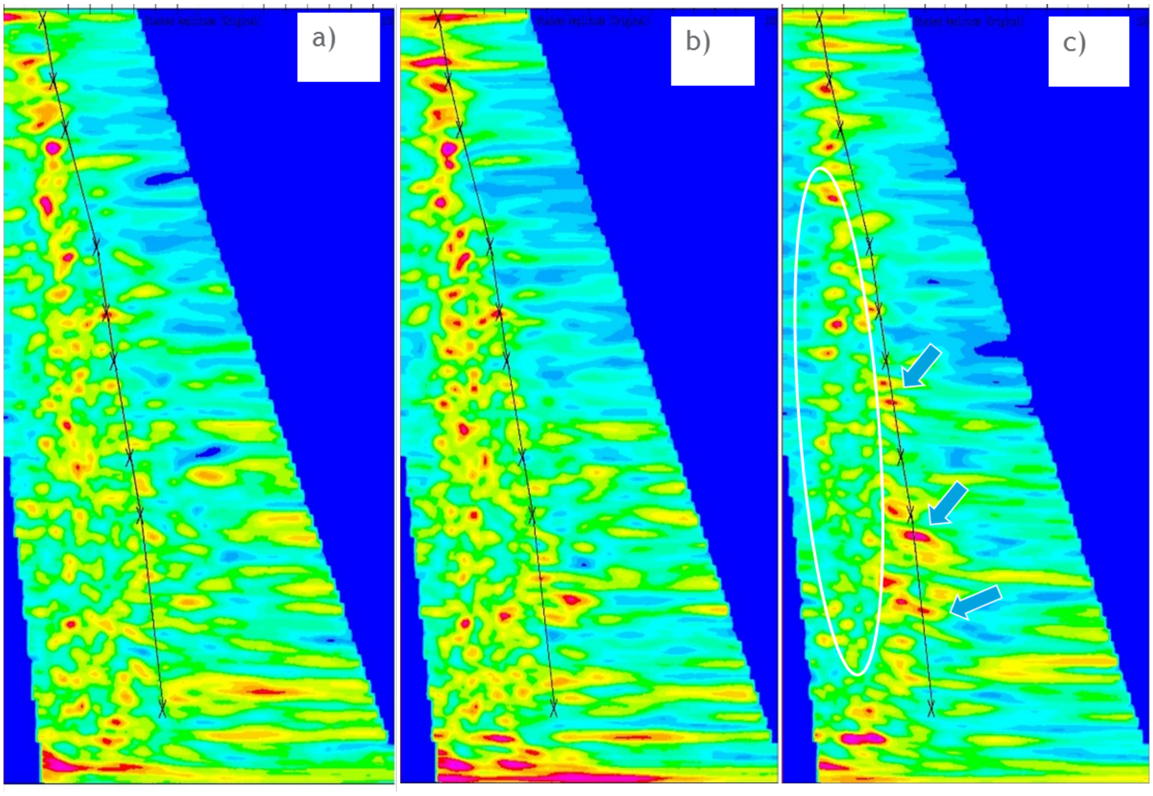

Figure 13 – Velocity semblance panels for (a) original data, (b) data after supergrouping, and (c) data after nonlinear beamforming. Black line shows the guide velocity function used during the beamforming process. White ellipse indicates a zone of suppressed multiples.

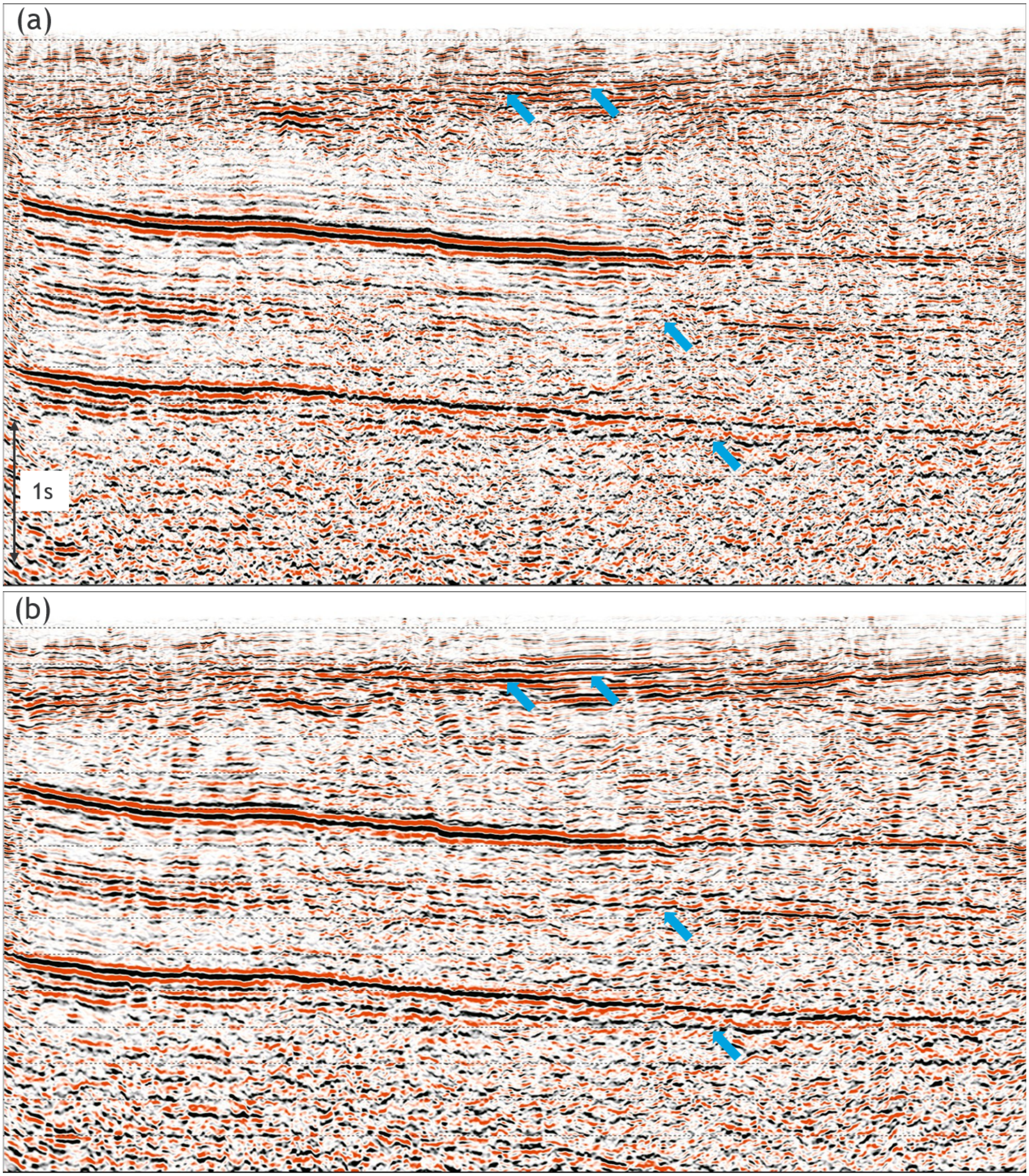

Figure 14 – Post-stack migration of data after (a) supergrouping 1x7, and (b) nonlinear beamforming.